aerospace

MDPI

Article

Experimental Evaluation of Lunar Regolith Settlement Caused by Ice Extraction

Zheng Gong [1], Nicholas Barnett [2], Jangguen Lee [3,*], Hyunwoo Jin [3], Byunghyun Ryu [3], Taeyoung Ko [4], Joung Oh [2], Andrew Dempster [2] and Serkan Saydam [2]

[1] Civil and Environmental Engineering, University of Science & Technology (UST-KICT School), ILsanseo-gu, Goyang-si 10233, Republic of Korea; gong@kict.re.kr

[2] School of Minerals and Energy Resources Engineering, University of New South Wales, Sydney 2052, Australia; nicholas.barnett@unsw.edu.au (N.B.); joung.oh@unsw.edu.au (J.O.); a.dempster@unsw.edu.au (A.D.); s.saydam@unsw.edu.au (S.S.)

[3] Department of Future and Smart Construction Research, Korea Institute of Civil Engineering and Building Technology (KICT), ILsanseo-gu, Goyang-si 10233, Republic of Korea; hyunwoo.jin@kict.re.kr (H.J.); tnt306@kict.re.kr (B.R.)

[4] Department of Energy and Resources Engineering, Kangwon National University, Gangwondaehak-gil, Chuncheon-si 24341, Republic of Korea; tyko@kangwon.ac.kr

* Correspondence: jlee@kict.re.kr; Tel.: +82-31-910-0791

Abstract: Water resources are essential to human exploration in deep space or the establishment of long-term lunar habitation. Ice discovered on the Moon may be useful in future missions to the lunar surface, necessitating the consideration of in situ resource utilization if it is present in sufficient amounts. Extraction of ice can cause the regolith to settle, which can lead to unintended structural damage. Therefore, any settlement resulting from ice extraction should be understood from a geotechnical perspective. This work reports on experimental investigation of the potential settlement caused by the extraction of ice from lunar regolith simulant containing different textures of ice. The KLS-1 simulant was prepared with different water contents and ice textures. Significant settlement occurred in simulant–ice mixtures with initial water contents of 5–10%.

Keywords: lunar ice; in situ resource utilization; regolith; water content; settlement; ice texture

check for updates

Citation: Gong, Z.; Barnett, N.; Lee, J.; Jin, H.; Ryu, B.; Ko, T.; Oh, J.; Dempster, A.; Saydam, S. Experimental Evaluation of Lunar Regolith Settlement Caused by Ice Extraction. *Aerospace* **2024**, *11*, 207. https://doi.org/10.3390/aerospace11030207

Academic Editor: Michael Nord

Received: 21 December 2023
Revised: 1 March 2024
Accepted: 4 March 2024
Published: 6 March 2024

1. Introduction

The concept of In Situ Resource Utilization (ISRU) was first extensively evaluated and studied at the Working Group on Extraterrestrial Resources (WGER) nearly 60 years ago, an informal organization of researchers and engineers interested in activities related to space resource utilization [1]. In early concepts for space habitats, the goal was to use water extracted on-site to sustain life or irrigate crops, and later as a source of energy for producing rocket fuel. Although detailed knowledge of the composition of the lunar soil was limited at the time, early concepts for the process of heating the regolith and extracting water were already in place [2]. The establishment of a long-term human presence in space must utilize extraterrestrial raw materials to reduce the need to transport resources from Earth. By utilizing space resources to provide materials required for space exploration, we can unleash the full potential of space exploration and greatly reduce the cost of space exploration. Similar to the extraction and use of terrestrial resources, to begin with, a given resource (e.g., oxygen, water ice) must be identified through prospecting and ground truthing to increase certainty [3]. NASA's report of the discovery of ice on the Moon in 1998 led to a later announcement in 2005 regarding the in situ utilization of lunar resources [4]. In recent research, the core concept of ISRU is using ice and volatile materials on the Moon to produce oxygen and water for exploration crews and provide propellant (rocket fuel) for deep space exploration [5–8]. This is consistent with earlier goals and patterns of ISRU.

Lunar ice and regolith are potential resources for life support, propellants, and mineral raw materials [9–13].

The Lunar Crater Observation and Sensing Satellite (LCROSS) found that the water content of lunar regolith in certain areas can be up to (5.6 ± 2.9)% [14]. A spacecraft Smart Lander for Investigating Moon (SLIM) from the Japan Aerospace eXploration Agency (JAXA) and the Indian Space Research Organization (ISRO) landed near the permanently shadowed regions (PSRs) at the lunar poles to conduct neutron, spectroscopic, and subsurface studies of possible water ice locations [15]. NASA and the European Space Agency (ESA) have also established and promoted ground exploration plans to observe the occurrence of lunar ice [16,17]. The data obtained to date show that ice exists at the Moon's shadowed polar craters [18], not only in the craters, but also in the surrounding cold traps [19–23]. International space agencies are preparing to explore lunar ice [24–26] by conducting activities such as sampling, drilling, and the collection and use of volatiles. While previous researchers have detected water ice on the Moon, the presence of water-rich regions containing (5.6 ± 2.9)% water content remains uncertain, necessitating quantitative investigations.

Lunar ice may manifest as small-grained water frost at the surface, as intricate mixtures of ice and regolith grains, or as subsurface ice layers. Johnson et al. [27] reported that lunar ice exists in various forms such as discrete ice, ice-coated or ice-cemented regolith, and ice breccia. Discrete ice is a physically mixed form of lunar regolith and ice, whereas ice-coated and ice-cemented regolith are physical combinations of lunar regolith and ice. Ice crystals are also expected in the form of embedded breccia.

Heating the lunar regolith appears to be a theoretically feasible means of extracting water [28,29]. Extracting water from ice under the lunar surface would leave a void, which is expected to lead to settlement owing to loads that include the weight of material above the void. Settlement represents a hazard, as it could overturn rovers or destabilize structures required for future ISRU. Therefore, thawing of icy layers near the surface can have substantial effects on lunar operations. Mechanical discontinuities in the substrate arising from water extraction on a slope may cause potentially destructive slides, flows, and slumps [30]. Establishing how much settlement to expect could aid the selection of resource extraction sites and the transport of resources across the lunar surface. Overall, designing structures and instruments that are resilient against expected settlement is crucial to ensure the safety and integrity of research and other activities on the Moon.

Despite the importance of engineering in withstanding settlement, no previous studies have investigated settlement due to ice extraction. Therefore, this work reports the investigation of settlement and behavior changes in regolith resulting from its alteration by compression and the heating of water ice in the regolith. Specimens of regolith simulant with varying water contents, ice textures, and loading conditions were compared. Extracting lunar water ice resources involves the phase transition of solid water ice to water vapor. However, conducting ice extraction in a vacuum environment to simulate lunar conditions poses experimental challenges. If the extraction occurs in a gaseous state rather than as water, it is anticipated that settlement resulting from ice extraction may be comparable to or even greater than that in atmospheric conditions due to an increase in void volume. In addition, during the experiment, the change in water content during the heating process was insignificant. This provides a more conservative estimation of settlement behavior, due to the expected increase in void volume if the ice water runs in the form of a gaseous state. The results are expected to help estimate settlement caused by ice extraction on the Moon.

2. Materials and Methods

2.1. Material

Simulant materials are required for the physical analysis of icy lunar regolith and the ground testing of payloads designed to be sent to the surface [31]. Lunar simulants are materials that simulate the physical, chemical, and mechanical properties of lunar regolith, which essentially comprises a layer of loose, heterogeneous, unconsolidated debris [32].

Given the scarcity of lunar regolith on Earth, studies must employ simulants with similar properties to real regolith [33,34]. The Korean Lunar Simulant (KLS-1) developed in 2015 was used in this study. KLS-1 validated the similarity of chemical, physical, and mechanical properties through comparative analysis with Apollo samples and common lunar simulants [35]. It has a similar mineral composition and particle size distribution to sampled lunar regolith (sample number 14163) [36] as well as other simulants, such as the Johnson Space Center simulant (JSC-1) and Fuji Japan Simulant (FJS-1), as shown in Figure 1. It also has similar physical and mechanical properties to JSC-1 and FJS-1 [35] (Table 1).

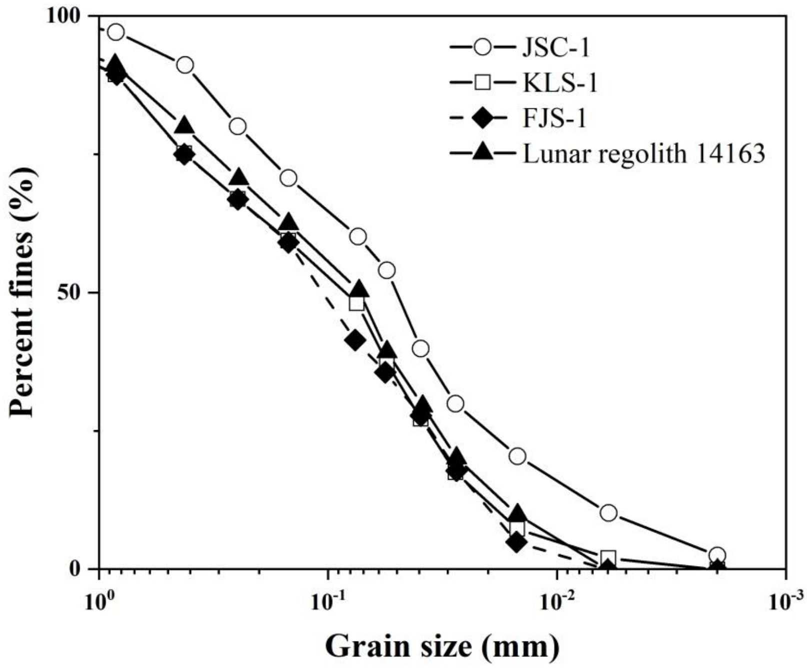

Figure 1. Particle size distributions of real lunar regolith and lunar simulants JSC-1, FJS-1, and KLS-1 [34].

Table 1. Mechanical properties of JSC-1, FJS-1, and KLS-1 lunar simulants.

lunar Simulant	Cohesion (kPa)	Friction Angle (°)	Specific Gravity (−)	Remarks
JSC-1	1.00	45.00	2.90	[37]
	1.65	45.00	2.92	[35]
FJS-1	3–8	32.5–39.4	2.94	[38]
	8.13	39.40	2.90	[35]
KLS-1	1.85	44.90	2.94	[35]

2.2. Experimental Apparatus

Figure 2 outlines the apparatus generally used in frozen ground engineering to test one-dimensional freezing and thawing. The mold had a height of 200 mm and an inner diameter of 200 mm; it comprised a 10 mm-thick acrylic material with low thermal conductivity. The outer area was covered with 400 mm-thick insulating extruded polystyrene. Ten temperature sensors (T-type thermocouples) ensured the reliability of temperature measurements inside the specimen. They were installed symmetrically at 20 mm intervals on the inner wall of the mold to allow observation of the vertical temperature distribution from 0 to 80 mm up the specimen. A linear variable displacement transducer (LVDT) with an accuracy of ±0.001 mm measured vertical displacement. Compression of the specimen (settlement) gave negative displacement values, and elevation of the sample (heaving) led to positive displacement values. The bottom temperature of the mold was controlled by a separate cooling pump. The upper part of the specimen was continually drained, with water extracted through the top surface, and an adjustable valve connected at the bottom of the mold allowed excess water to drain from the specimen. The experiment was carried out in a large refrigerated room to control atmospheric temperature, and the internal temperature of the specimen was carefully controlled using a temperature controller at the bottom.

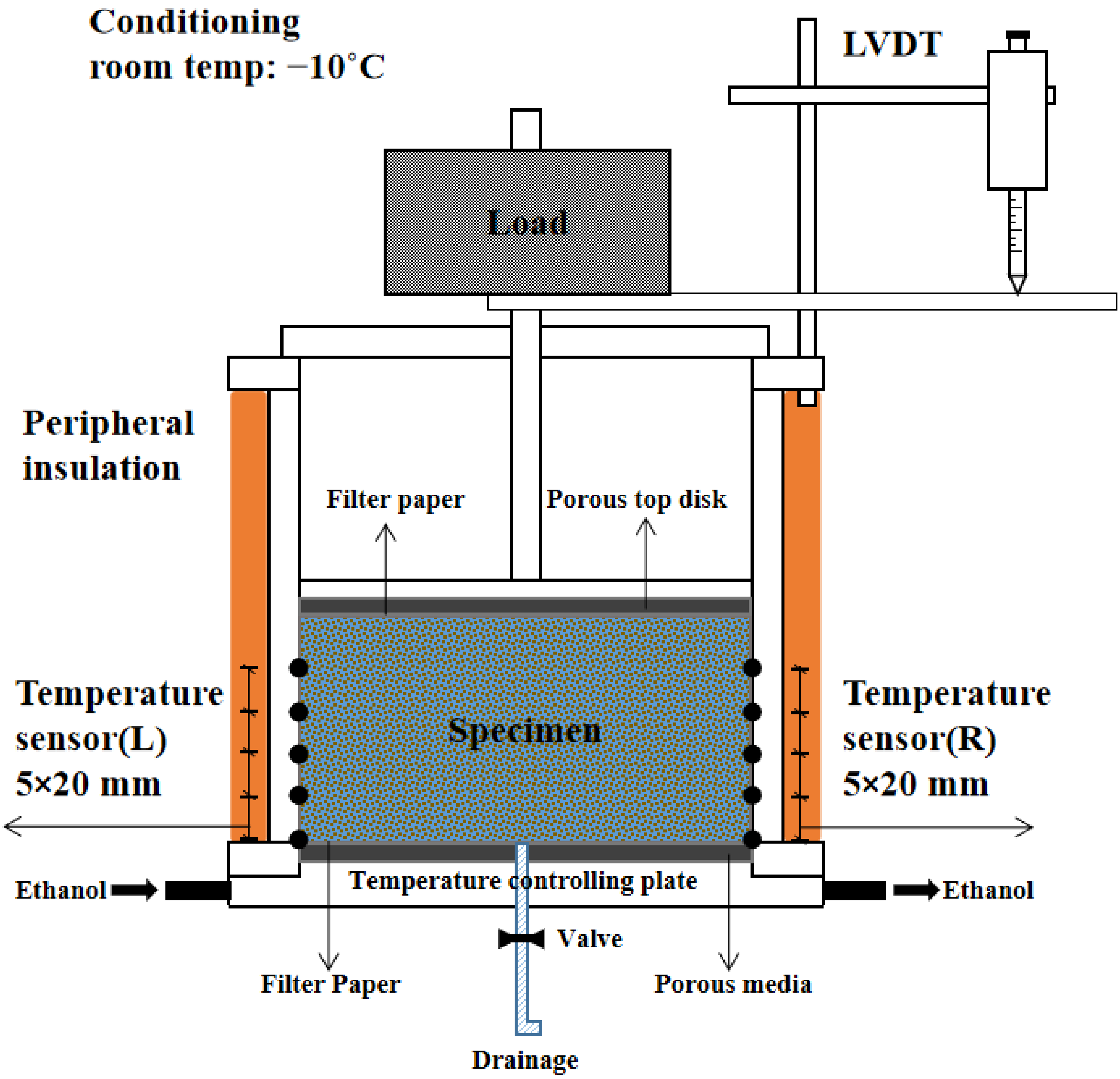

Figure 2. Schematic diagram of lunar simulant thawing testing apparatus.

2.3. Specimen Preparation and Testing Method

A standard heating procedure (110 °C for 24 h) first removed any initial moisture from KLS-1 [39]. The dried regolith simulant was then used to prepare unsaturated frozen specimens with target initial water contents of 1%, 5%, and 10%. Gravimetric analysis confirmed the actual water content: a sample of each mixture was weighed before and after drying in an oven at 110 °C for 24 h, and the mass loss was calculated. Three different types of frozen samples were prepared to reproduce unsaturated lunar permafrost with different physical textures; NASA reports that the surface gravity of the Moon is approximately 1.62 m/s^2, which is roughly one-sixth of Earth's. To simulate human weight on the Moon, a pressure of 4.2 kPa is required for a mass of 13.5 kg on Earth and 80 kg on the Moon. Similarly, a pressure of 10.2 kPa is required to simulate a lunar rover with a mass of 200 kg. According to the Apollo 17 mission, each Lunar Roving Vehicle (LRV) has a mass of 210 kg without payload [40]. For engineering safety purposes, a more conservative pressure is adopted. Therefore, the samples were classified into two groups for testing using two different overburden pressures (Table 2). In addition, porosity serves as a crucial indicator for representing soil structure; however, testing specimens in an unsaturated state poses challenges in directly measuring porosity. Instead, dry unit weight can be directly measured, which is a reliable indicator of porosity. As dry unit weight increases, porosity decreases. In this case, Table 2 records the dry unit weight of the sample.

Table 2. Specimen initial conditions.

CASE	Overburden Pressure (kPa)	Specimen Mass (g)	Water Content (%)	Height (mm)		Soil Mass (g)	Water Mass (g)	Dry Unit Mass (kN/m^3)
	P	W_t	w_i	H_0	H_i	W_s	W_w	γ_d
I-1-1	4.2	4927.3	11.3	120.7	119.1	4415.1	498.9	11.6
I-1-2		5468.0	4.9	112.3	111.3	5212.6	255.4	14.6
I-1-3		5585.0	1.3	106.3	106.1	5513.3	71.67	16.2
II-1-1		4350.0	10.6	115.3	114.2	3933.1	416.9	10.8
II-1-2		4288.3	10.6	118.7	116.1	3887.9	412.1	10.5
III-1		4941.5	10.0	110.7	110.9	4496.4	449.6	12.7
I-2-1	10.4	4936.1	11.3	119.0	116.5	4415.1	498.9	11.9
I-2-2		5482.2	4.9	114.0	111.9	5221.2	255.8	14.6
I-2-3		5751.0	1.3	109.0	106.7	5677.2	73.8	16.6
II-2-1		4346.1	10.6	115.7	112.5	3933.9	416.9	10.9
II-2-2		4262.4	10.6	119.7	116.7	3864.4	409.6	10.3
III-2		5293.9	9.9	121.0	120.8	4821.5	477.3	12.5

Samples for cases I and II were prepared in a large refrigerated room maintained at −10 °C. The case I samples comprised KLS-1 and fine ice particles (up to 0.225 mm) that were physically mixed as discrete ice. The ice used in the experiments was prepared using distilled water in another small freezer in a separate laboratory. The small freezer isolated the area surrounding the ice, minimizing the influence of outside temperature, and induced one-dimensional freezing from bottom to top. Ice was generated by slow one-dimensional freezing for about 48 h to remove as many dissolved air bubbles as possible from the distilled water during its phase transition to ice [41]. Finally, the ice was crushed, and a sieve was used to select particles up to 0.225 mm. The case II samples comprised physical combinations of lunar regolith and ice (ice-coated or ice-cemented regolith). Therefore, after mixing distilled water with dried KLS-1 and then freezing in the large refrigerated room for 24 h, the mixture was pulverized and sieved to collect particles of up to 0.850 mm. After preparing the case I and II samples, they were poured into the undrained mold based on the calculated weight, and the height (*Ho*) was obtained. After each experiment was set up, the temperature inside each specimen was conditioned using the bottom temperature controller set to −5 °C. During the initial temperature conditioning, the specimen was consolidated by simultaneously applying an overburden pressure (P). Settlement caused by the consolidation was measured and was considered complete when the LVDT readings no longer changed significantly (the consolidation rate was <0.01 mm per 1 h) after standing the sample for at least 4 h. The initial temperature condition at −5 °C and the height (Hi) of the fully consolidated specimen were set as initial conditions.

The case III samples, comprising KLS-1 mixed with distilled water, were poured into the mold and consolidated in the large refrigerated room maintained at 10 °C. When the consolidation was completed, the temperature of the room was decreased to −10 °C, and the bottom temperature controller was also set to −10 °C. As each specimen froze, a small degree of frost heave occurred. This was completed when the internal temperature of the specimen was below 0 °C. The temperature and specimen height (Hi) in this state were regarded as the initial conditions.

After completing specimen conditioning, both the temperature in the large refrigerated room and the bottom temperature controller increased simultaneously to facilitate the melting of ice, and the bottom valve was opened. The settlement caused by the ice thawing was measured, and the test was considered complete when the LVDT readings no longer changed significantly (i.e., the consolidation rate of the specimen was <0.01 mm per 1 h).

3. Results

The experimental results are grouped by overburden pressure (4.2 or 10.4 kPa). In total, there are 12 experimental results for the tested pressures and specimen types. This division is intended to facilitate discussion of the results.

3.1. Initial Water Content and Overburden Pressure

Case I specimens with varying water contents were tested under differing overburden pressures. The results in Figure 3 include the temperature change of the upper (80 mm), middle (40 mm), and bottom (0 mm) section of each specimen. Initial settlement occurred owing to the applied overburden pressure, and it increased with increasing overburden pressure. Thawing began after consolidation caused by the overburden pressure, and the settlement increased with increasing initial water content and overburden pressure. Settlement was relatively small at an initial water content of 1.3%, but significant settlement occurred when the water content was greater than 5%.

The settlement ratio (SR) is the ratio of the total change in height ($\Delta H = Hi - Hf$) to the initial specimen height (Hi), calculated as $\Delta H/H_i$ (Table 3), and increased with increasing initial water content (Figure 4). When the initial water content exceeded 5%, SR became significant and increased with increasing overburden pressure. The settlement ratio reached 6.68% for an overburden pressure of 4.2 kPa, whereas 10.39% was obtained at 10.4 kPa. Figure 5 shows that the dry unit weight of specimens with 5% initial water content changed little after testing. Specimens with 11% initial water content showed a pronounced change in dry unit weight. In contrast, water content did not differ significantly after the experiment, regardless of the test conditions (Figure 6). After each experiment, the bottom drainage was checked, and no water was collected.

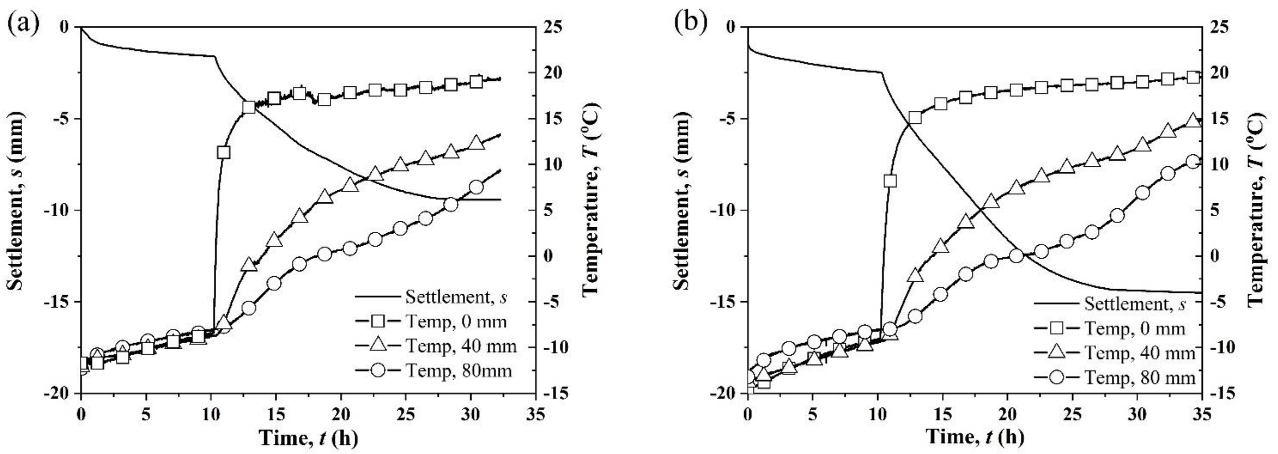

Figure 3. *Cont.*

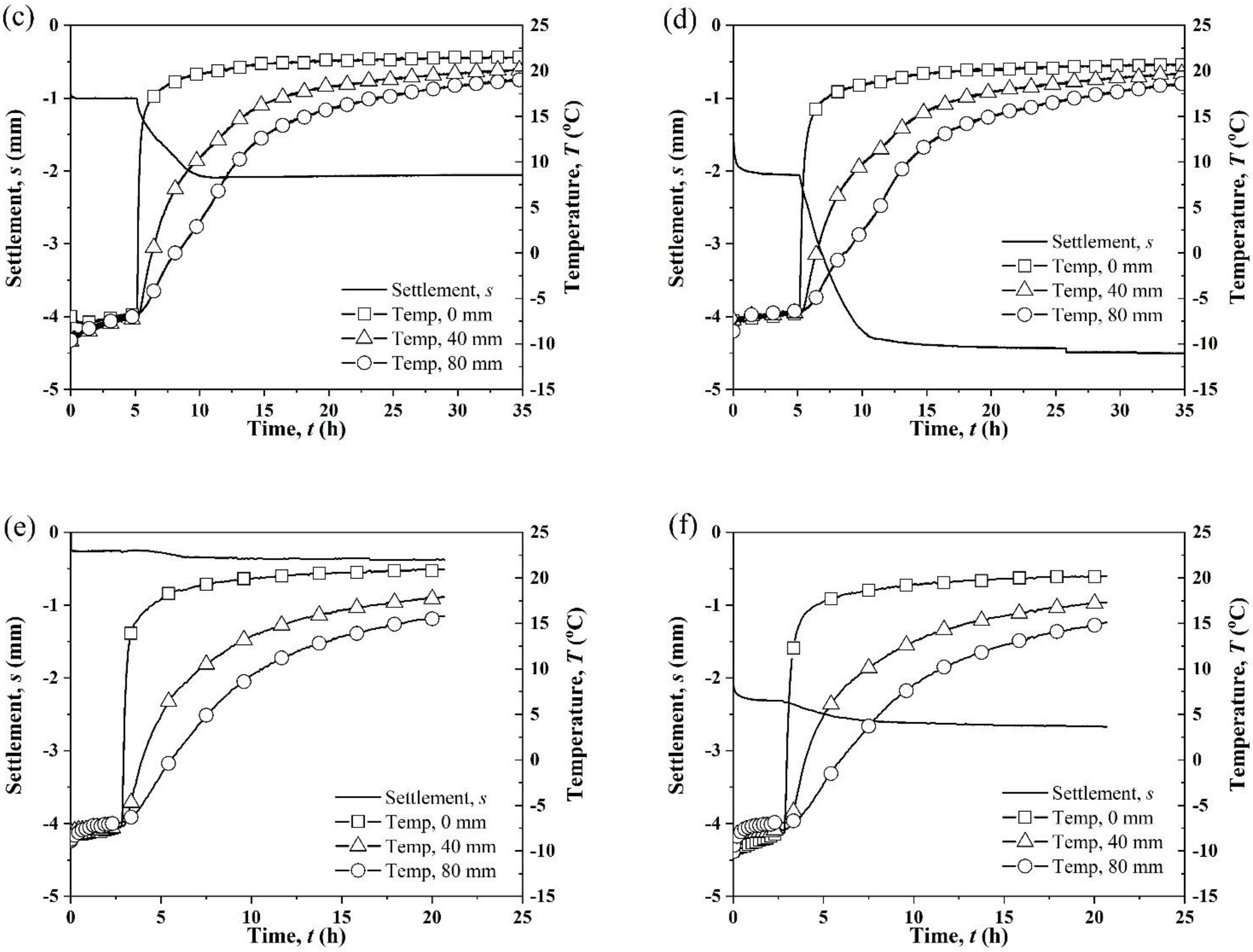

Figure 3. Measured settlement and temperature profiles for case I specimens: (**a**) I-1-1, (**b**) I-2-1, (**c**) I-1-2, (**d**) I-2-2, (**e**) I-1-3, and (**f**) Case I-2-3.

Table 3. Measured initial and final results for case I specimens.

Case	Overburden Pressure (kPa)	Water Content (%)		Specimen Height (mm)		Measured Settlement (mm)	Settlement Ratio (%)	Dry Unit Weight γ_d (kN/m^3)	
	P	w_i	w_f	H_i	H_f	s	SR	Initial	Final
I-1-1	4.2	11.3	11.6	119.1	111.2	7.95	6.68	11.6	12.4
I-1-2		4.90	4.80	111.3	110.3	1.00	0.90	14.6	14.8
I-1-3		1.30	1.20	106.1	106.0	0.10	0.09	16.2	16.2
I-2-1	10.4	11.3	11.8	116.5	104.4	12.10	10.39	11.8	13.2
I-2-2		4.90	5.00	111.9	109.5	2.40	2.14	14.6	14.9
I-2-3		1.30	1.30	106.7	106.3	0.40	0.37	16.6	16.7

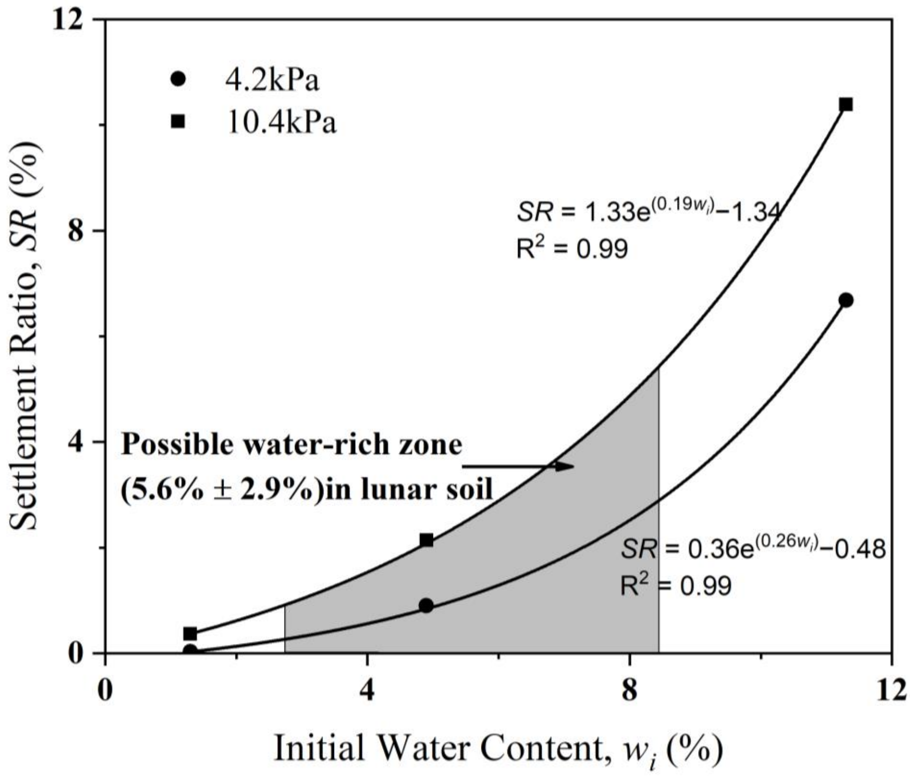

Figure 4. Settlement ratio with respect to the regolith simulant's initial water content under different loading conditions for case I specimens.

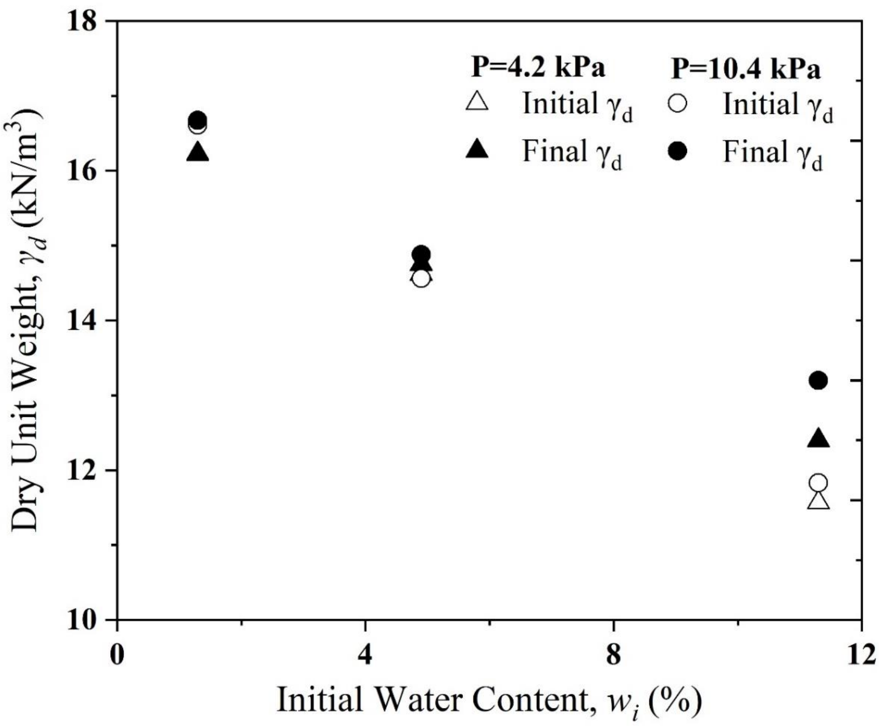

Figure 5. Change in dry unit weight caused by thawing case I specimens.

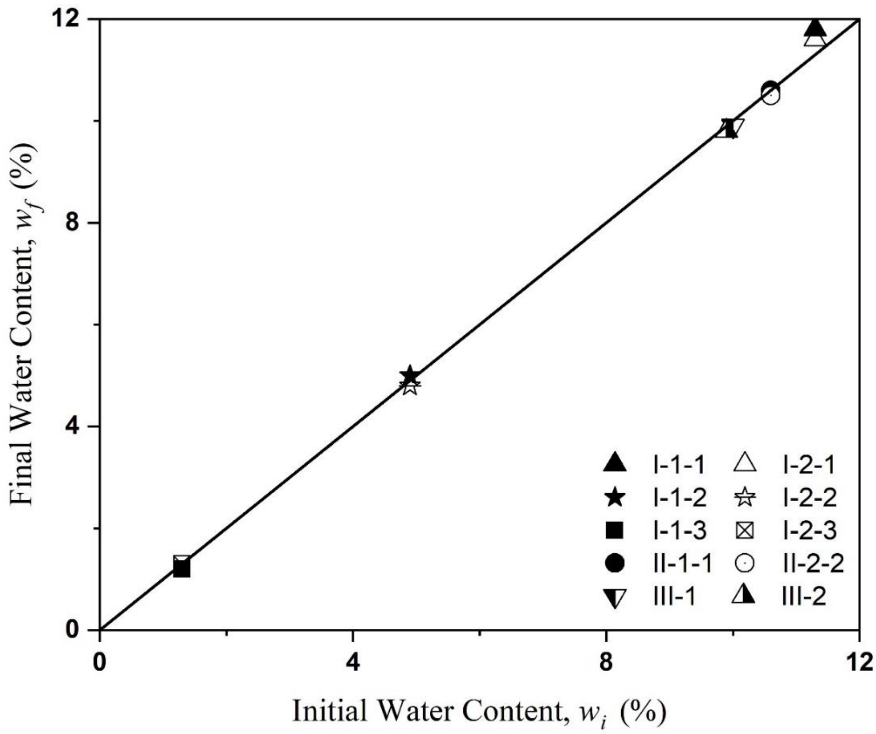

Figure 6. Change in water content for all cases.

3.2. Ice Texture

Table 4 lists the experimental conditions and results for all specimens. The case II specimens showed the largest total settlement, under both tested overburden pressures: settlement reached 14.8 and 20.3 mm at 4.2 and 10.4 kPa, respectively (Figure 7a,b), leading to settlement ratios of 12.8% and 17.4%, respectively. In contrast, the case III specimens had minimal settlement, with 0.2 and 1.6 mm at 4.2 and 10.4 kPa, respectively, yielding settlement ratios of 0.18% and 1.33%, respectively (Figure 7c,d).

Table 4. Measured initial and final results with estimated settlement for case I, II, and III specimens.

Case	Overburden Pressure (KPa)	Water Content (%)		Specimen Height (mm)		Measured Settlement (mm)	Settlement Ratio (%)	Calculated Settlement [1] (mm)	Dry Unit Weight γ_d (kN/m^3)	
	P	w_i	w_f	H_i	H_f	s	SR		Initial	Final
I-1-1	4.2	11.3	11.6	119.1	111.2	7.95	6.68	1.43	11.6	12.4
II-1-1		10.6	10.6	114.2	101.6	12.60	11.03	1.19	10.8	12.1
II-1-2		10.6	10.3	116.1	101.3	14.80	12.75	1.18	10.5	12.0
III-1		10.0	9.90	110.7	110.7	0.17	0.09	1.29	12.7	12.7
I-2-1	10.4	11.3	11.8	116.5	104.4	12.10	11.03	1.43	11.8	13.2
II-2-2		10.6	10.5	112.5	95.5	17.00	15.11	1.19	10.9	12.9
II-2-2		10.6	10.3	116.7	96.4	20.30	17.40	1.17	10.3	12.5
III-2		9.90	9.80	120.8	119.2	1.60	1.32	1.37	12.5	12.6

[1] Calculated using Equation (1).

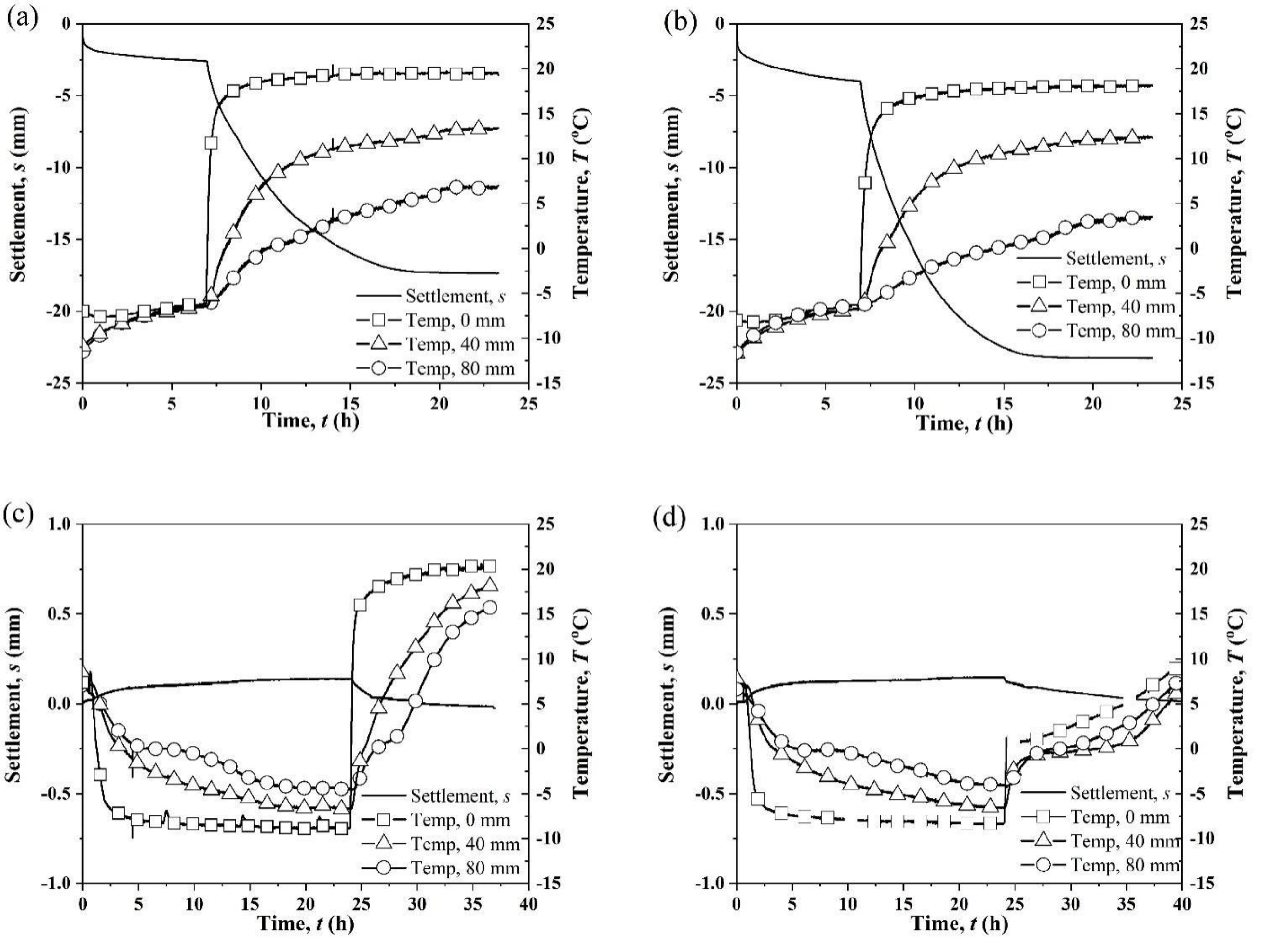

Figure 7. Measured settlement and temperature profiles for case II and III specimens: (**a**) II-1-2, (**b**) II-2-1, (**c**) III-1, and (**d**) III-2.

Frost heave might have occurred during freezing of the case III specimens (Figure 7c,d), but this is likely to have been minimal (~0.2 mm). This frost heave was attributed to volume expansion during the phase change of pore water to ice. Afterwards, the bottom temperature controller was raised to 10 °C. The resulting settlement was insignificant and similar to the heave amount.

4. Discussion

4.1. Ice Content and Overburden Pressure

The settlement ratio was positively related to the initial ice content (i.e., water content), as shown in Figure 4. Even when only considering the range of ice contents of lunar regolith (5.6 ± 2.9)%, non-negligible settlement ratios (>3%) occurred under a relatively small overburden pressure of 4.2 kPa. Figure 5 shows that 5% ice content is a threshold at which there is a noticeable change in dry unit weight, which is similar to the trend in Figure 4. When the initial water content exceeded 5%, the settlement ratio became significant, and even reached 10% under 10.4 kPa. This represents a serious engineering consideration when planning works in ice-rich areas of the Moon. Figures 4 and 5 show that when the dry unit weight changed significantly, the settlement ratio also increased rapidly. However, Figure 6 shows that the initial and final moisture contents were similar. This indicates that the increase in settlement is not related to drainage conditions when the initial water content is below 10%.

4.2. Settlement Caused by Structural Change

The approximately 9% volume change of water as it changes phase must also be considered as a factor affecting the settlement ratio [42]. Based on the initial water content, the amount of settlement (*Sm*, mm) due to ice melting was calculated using Equation (1):

$$Sm = (V_w/A) \times 0.09, \tag{1}$$

where V_w is the initial volume of water (mm^3) in the specimen, and A is the cross-sectional area (mm^2). As a result, the predicted settlement amount induced by ice melting for all cases was approximately 1.18 to 1.43 mm. These amounts are insignificant compared with the measured settlements. Therefore, the total thawing settlement was dominated by changes in the soil structure, rather than the phase change of ice melting or the escape of meltwater. In particular, the case III specimens showed insignificant frost heave during freezing and insignificant settlement during thawing. This was because the pore spaces could accommodate any volume change during phase changes in the unsaturated specimen. Therefore, even during thawing, the framing structure of soil particles showed minimal change, leading to insignificant settlement. This phenomenon is well represented by the insignificant change in dry unit weight before and after the test (Table 4), despite the specimen undergoing freezing and thawing. This means that the structure of the soil remained unchanged.

4.3. Ice Texture

The case II specimens, which comprised lunar simulant particles coated with ice, yielded the poorest results. The settlement ratios were approximately 40% higher than those of the case I specimens. The measured dry unit weights (γ_d) of the case II specimens were lower than those of the case I specimens with similar initial water content (w_i). This could have been caused by the particles being composed of both lunar regolith simulant and ice. That is, the physically ice-bonded particles had a relatively large volume at a given weight, and ice particles played a role similar to soil particles, so the dry unit weight was low. Therefore, during thawing process, the ice covering the simulant particles melted, leading to an increase in sample porosity. This, in turn, contributed to settlement, resulting in a relatively large settlement. This was demonstrated by the similar dry unit weights of the case I and II specimens after the completion of the final thawing settlement. Even after the completion of thawing, the change in water content in the sample was negligible, and no water was collected in the bottom drainage after each heating. Therefore, settlement due to pore water escape was not significant.

5. Conclusions

Lunar ice will be an important resource for deep space exploration and long-term extraterrestrial presence. Various space agencies are planning extraterrestrial missions, which could be greatly aided by ISRU. Lunar ice is expected to facilitate the operation of a manned lunar base. However, ground settlement following ice extraction is a potential geotechnical hazard and has not been evaluated in a lunar context. The experiments conducted here assessed settlement following the thawing of ice in lunar regolith and led to the following conclusions.

(1) At the same pressure level, an initial water content of approximately 5% appears to be a critical threshold. Beyond this threshold, when the water content reaches approximately 10%, even a relatively small overburden pressure of 4.2 kPa can lead to settlement ratios ranging from 6.68% to 12.75%. For the water contents of lunar regolith (5.6 $\pm$ 2.9)%, the settlement ratio may reach around 5%. Therefore, care must be taken when extracting ice from water-rich unsaturated lunar regolith ice layers.

(2) Based on existing research and assumptions, this study reproduced three structures of ice-bearing lunar regolith and examined the amount of settlement due to extraction of the ice. Ice-coated or ice-cemented regolith (case II) showed the greatest settlement.

The smallest initial dry unit weight of case II explains this phenomenon. When relatively large ice-regolith agglomerates melt, porosity increases along with void volume, leading to the largest settlement and the largest change in dry unit weight under pressure. However, if lunar ice exists as ice breccia containing ice crystals, the amount of settlement due to its extraction is expected to be insignificant.

Author Contributions: Conceptualization, Z.G. and N.B.; methodology, J.L., N.B. and Z.G.; equipment preparation and modification: B.R. and J.L.; software, Z.G.; validation, Z.G. and N.B.; formal analysis, Z.G.; investigation, Z.G.; data curation, Z.G.; writing—original draft preparation, Z.G.; writing—review and editing, J.L., H.J. and T.K.; visualization, Z.G.; supervision, J.L., J.O., A.D. and S.S.; project administration, J.L. All authors have read and agreed to the published version of the manuscript.

Funding: This research was funded by Korea Institute of Construction Technology (KICT). Research for this paper was carried out under the KICT Research Program (project no. 20220124, Development of Environmental Simulator, and Advanced Construction Technologies over TRL6 in Extreme Conditions) and was funded by the Ministry of Science and ICT.

Data Availability Statement: The data that support the findings of this study are available from the corresponding author upon reasonable request.

Conflicts of Interest: The authors declare that they have no known competing financial interests or personal relationships that could have appeared to influence the work reported in this paper.

References

1. Meurisse, A.; Carpenter, J. Past, present and future rationale for space resource utilisation. *Planet. Space Sci.* **2020**, *182*, 104853. [CrossRef]
2. Johnson, G.W.S. A report of the working group on extraterrestrial resources. In *Astronautics Information: Recommendations for Utilization of Lunar Resources*; Jet Propulsion Lab., California Inst. of Tech.: Pasadena, CA, USA, 1963.
3. Cilliers, J.; Hadler, K.; Rasera, J. Toward the utilisation of resources in space: Knowledge gaps, open questions, and priorities. *Npj Microgravity* **2023**, *9*, 22. [CrossRef]
4. Jayathilake, B.A.C.S.; Ilankoon, I.M.S.K.; Dushyantha, M.N.P. Assessment of significant geotechnical parameters for lunar regolith excavations. *Acta Astronaut.* **2022**, *196*, 107–122. [CrossRef]
5. Anand, M.; Crawford, I.A.; Balat-Pichelin, M.; Abanades, S.; van Westrenen, W.; Péraudeau, G.; Jaumann, R.; Seboldt, W. A brief review of chemical and mineralogical resources on the Moon and likely initial in situ resource utilization (ISRU) applications. *Planet. Space Sci.* **2012**, *74*, 42–48. [CrossRef]
6. Kaschubek, D.; Killian, M.; Grill, L. System analysis of a Moon base at the south pole: Considering landing sites, ECLSS and ISRU. *Acta Astronaut.* **2021**, *186*, 33–49. [CrossRef]
7. Sanders, G.B.; Larson, W.E. Progress Made in Lunar In Situ Resource Utilization under NASA's Exploration Technology and Development Program. *J. Aerosp. Eng.* **2013**, *26*, 5–17. [CrossRef]
8. Larson, W.E.; Picard, M.; Colaprete, A.; Sanders, G.B.; Elphic, R.C. RESOLVE: Ground truth for polar volatiles as a resource. In Proceedings of the 62nd International Astronautical Congress Conference/International Astronautical Federation, Cape Town, South Africa, 3–7 October 2011; NASA Kennedy Space Center: Cocoa Beach, FL, USA, 2011.
9. Radl, A.; Neumann, K.M.; Wotruba, H.; Clausen, E.; Friedrich, B. From lunar regolith to oxygen and structural materials: An integrated conceptual design. *CEAS Space J.* **2023**, *15*, 585–595. [CrossRef]
10. Guerrero-Gonzalez, F.J.; Zabel, P. System analysis of an ISRU production plant: Extraction of metals and oxygen from lunar regolith. *Acta Astronaut.* **2023**, *203*, 187–201. [CrossRef]
11. Stoeser, D.; Rickman, D.; Wilson, S. Design and Specifications for the Highland Regolith Prototype Simulants NU-LHT-1M and-2M. 2010. Available online: https://www.lpi.usra.edu/lunar/samples/2010_216438.pdf (accessed on 16 November 2023).
12. Ellery, A. Sustainable in-situ resource utilization on the Moon. *Planet. Space Sci.* **2020**, *184*, 104870. [CrossRef]
13. Taylor, L.A.; Carrier, W.D. Production of Oxygen on the Moon: Which Processes Are Best and Why. *AIAA J.* **1992**, *30*, 2858–2863. [CrossRef]
14. Colaprete, A.; Schultz, P.; Heldmann, J.; Wooden, D.; Shirley, M.; Ennico, K.; Hermalyn, B.; Marshall, W.; Ricco, A.; Elphic, R.C.; et al. Detection of water in the LCROSS ejecta plume. *Science* **2010**, *330*, 463–468. [CrossRef] [PubMed]
15. Hoshino, T.; Wakabayashi, S.; Ohtake, M.; Karouji, Y.; Hayashi, T.; Morimoto, H.; Shiraishi, H.; Shimada, T.; Hashimoto, T.; Inoue, H.; et al. Lunar polar exploration mission for water prospection—JAXA's current status of joint study with ISRO. *Acta Astronaut.* **2020**, *176*, 52–58. [CrossRef]
16. Feder, J. NASA Prepares to Drill for the "Oil of Space". *J. Pet. Technol.* **2021**, *73*, 24–28. [CrossRef]

17. Heinicke, C.; Foing, B. Human habitats: Prospects for infrastructure supporting astronomy from the Moon. *Philos. Trans. R. Soc. A Math. Phys. Eng. Sci.* **2021**, *379*, 20190568. [CrossRef] [PubMed]
18. Hayne, P.O.; Hendrix, A.; Sefton-Nash, E.; Siegler, M.A.; Lucey, P.G.; Retherford, K.D.; Williams, J.-P.; Greenhagen, B.T.; Paige, D.A. Evidence for exposed water ice in the Moon's south polar regions from Lunar Reconnaissance Orbiter ultraviolet albedo and temperature measurements. *Icarus* **2015**, *255*, 58–69. [CrossRef]
19. Cocks, F. Lunar Ice: Adsorbed Water on Subsurface Polar Dust. *Icarus* **2002**, *160*, 386–397. [CrossRef]
20. Duke, M.B. Lunar polar ice deposits: Scientific and utilization objectives of the Lunar Ice Discovery Mission proposal. *Acta Astronaut.* **2002**, *50*, 379–383. [CrossRef]
21. Hodges, R.R. Ice in the lunar polar regions revisited. *J. Geophys. Res. Planets* **2002**, *107*, 6-1–6-7. [CrossRef]
22. Anand, M. Lunar Water: A Brief Review. *Earth Moon Planets* **2011**, *107*, 65–73. [CrossRef]
23. Cannon, K.M.; Britt, D.T. A geologic model for lunar ice deposits at mining scales. *Icarus* **2020**, *347*, 113778. [CrossRef]
24. Nasa. NASA's Management of the Orion Multi-Purpose Crew Vehicle Program. 2020. Available online: https://oig.nasa.gov/docs/IG-20-018.pdf (accessed on 16 November 2023).
25. ESA Strategy for Science at the Moon. 2019. Available online: https://sci.esa.int/documents/34161/35992/1567260389633-ESA_Strategy_for_Science_at_the_Moon.pdf%20 (accessed on 16 November 2023).
26. International Space Exploration Coordination Group (ISECG). Scientific Opportunities Enabled by Human Exploration Beyond Low-Earth Orbit. 2018. Available online: https://www.globalspaceexploration.org/wordpress/wp-content/isecg/ISECG%20SWP_FINAL-web_2017-12.pdf (accessed on 16 November 2023).
27. Johnson, D.K.M.; Dreyer, C.B.; Cannon, K.M.; Sowers, G. Pressure Sintered icy lunar regolith Simulant (PSS): A novel icy regolith simulant production method. *Icarus* **2024**, *410*, 115885. [CrossRef]
28. Sowers, G.F.; Dreyer, C.B. Ice Mining in Lunar Permanently Shadowed Regions. *New Space* **2019**, *7*, 235–244. [CrossRef]
29. Cole, J.D.; Lim, S.; Sargeant, H.M.; Sheridan, S.; Anand, M.; Morse, A. Water extraction from icy lunar simulants using low power microwave heating. *Acta Astronaut.* **2023**, *209*, 95–103. [CrossRef]
30. Nelson, F.E.; Anisimov, O.A.; Shiklomanov, N.I. Subsidence risk from thawing permafrost. *Nature* **2001**, *410*, 889–890. [CrossRef] [PubMed]
31. Liu, J.; Zhang, W.; Cui, J.; Ren, Z.; Wang, E.; Li, X.; Wei, G.; Tian, Y.; Ji, J.; Ma, J.; et al. Extreme low-temperature freezing process and characteristic curve of icy lunar regolith simulant. *Acta Astronaut.* **2023**, *202*, 485–496. [CrossRef]
32. Nasa. Lunar Rocks and Soils from Apollo Missions. 2023. Available online: https://curator.jsc.nasa.gov/lunar/ (accessed on 16 November 2023).
33. Edmunson, J.; Betts, W.; Rickman, D.; Mclemore, C.; Fikes, J.; Stoeser, D.; Wilson, S.; Schrader, C. NASA lunar regolith simulant program. In Proceedings of the Lunar and Planetary Science Conference, Marshall Space Flight Center, The Woodlands, TX, USA, 1–5 March 2010.
34. Ryu, B.-H.; Baek, Y.; Kim, Y.-S.; Chang, I. Basic Study for a Korean Lunar Simulant (KLS-1) Development. *J. Korean Geotech. Soc.* **2015**, *31*, 53–63. [CrossRef]
35. Ryu, B.-H.; Wang, C.-C.; Chang, I. Development and Geotechnical Engineering Properties of KLS-1 Lunar Simulant. *J. Aerosp. Eng.* **2018**, *31*, 04017083. [CrossRef]
36. Schnetzler, C.C.; Nava, D.F. Chemical composition of Apollo 14 soils 14163 and 14259. *Earth Planet. Sci. Lett.* **1971**, *11*, 345–350. [CrossRef]
37. Willman, B.M.; Boles, W.W.; Mckay, D.S.; Allen, C.C. Properties of lunar soil simulant JSC-1. *J. Aerosp. Eng.* **1995**, *8*, 77–87. [CrossRef]
38. Kanamori, H.; Udagawa, S.; Yoshida, T.; Matsumoto, S.; Takagi, K. Properties of lunar soil simulant manufactured in Japan. *Space* **1998**, *98*, 462–468. [CrossRef]
39. *ASTM D 4643-17*; Standard Test Method for Determination of Water Content of Soil and Rock by Microwave Oven Heating. ASTM International: West Conshohocken, PA, USA, 2017.
40. Baker, D. Lunar Roving Vehicle: Design Report. *Spaceflight* **1971**, *13*, 234–240.
41. Jin, H.; Lee, J.; Zhung, L.; Ryu, B.H. Laboratory investigation of unconfined compression behavior of ice and frozen soil mixtures. *Geomech. Eng.* **2022**, *22*, 219–226. [CrossRef]
42. Lackner, R.; Amon, A.; Lagger, H. Artificial ground freezing of fully saturated soil. *J. Eng. Mech.* **2005**, *131*, 211–220. [CrossRef]